

ABSOLUTE TRANSIT TIME DETECTION FOR ULTRASONIC GAS FLOWMETERS BASED ON TIME AND PHASE DOMAIN CHARACTERISTICS

Mario Kupnik^{*}, Edwin Krasser[†], and Martin Gröschl[‡]

^{*}Edward L. Ginzton Laboratory, Stanford University, Stanford, CA-94305-4088, USA

[†]Institute of Electronics, Graz University of Technology, A-8010, Austria

[‡]Institute of General Physics, Vienna University of Technology, A-1040, Austria

Abstract—We present an absolute transit time detection algorithm for ultrasonic gas flowmeters (UFMs). The major objective is a reliable and accurate detection, even when the received signals experience a change and degradation of their shape. This can be due to parasitic effects, such as high gas temperatures and pressure fluctuations. We employ a time and phase domain based detection algorithm that determines the absolute transit times independently for the upstream and downstream channel. The Hilbert transform is applied to calculate the wrapped phase signal; each section of this phase signal is analyzed step-by-step. The algorithm was tested on real measurement data obtained from a double-path UFM (wetted configuration using capacitive ultrasonic transducers) installed at the end of an exhaust gas train of an automotive combustion engine. Over a gas temperature range of 400°C and a mass flow range of 163 kg/h, corresponding to a signal-to-noise ratio (SNR) range from 18 to 8 dB, all transit times were detected correctly, *i.e.* without any cycle skip. Further, our results show that the algorithm outperforms cross-correlation methods in terms of the absolute transit time detection.

I. INTRODUCTION

The accuracy and applicability of ultrasonic sensors [1], and in particular of ultrasonic transit time gas flowmeters [2, 3], mainly depend on the performance and reliability of the transit time detection algorithm.

For ultrasonic transit time gas flowmeters two kinds of time information need to be evaluated to determine the gas flow velocity and sound velocity: First, the relative time difference Δt of the arrival times in the upstream and downstream channel. Depending on the particular application and geometry of the UFM, this time difference may need to be resolved in the ns or sub ns range; Second, the absolute transit times (t_{up} , t_{down}), *i.e.* the durations the ultrasonic pulses propagate from the transmitter to the receiver in the upstream and downstream channel, respectively. This absolute transit times, which range in the several (hundred) μs range, mainly depend on the pipe diameter and gas temperature, for a given gas.

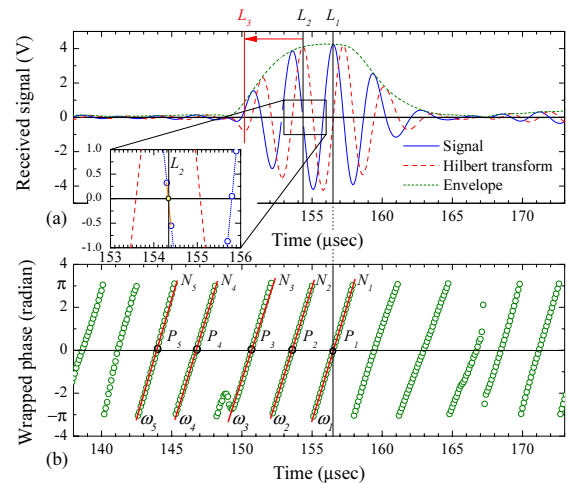


Fig. 1. Exemplary visualization of the working principle of the time (a) and phase domain (b) based algorithm (Fig. 2), by using a received ultrasonic time signal.

Capacitive ultrasonic transducers (CUTs) have been shown to be advantageous for wetted UFM configurations [4]. Due to their broadband behavior (fractional bandwidth of $\sim 100\%$) and good match of acoustic impedance to the gas, high pulse repetition frequencies (PRFs) allow the realization of UFMs, capable to measure transients in the gas flow [5]. Further improvements of CUTs, in terms of their applicability to higher gas temperatures [6], opened the door to new applications, such as the measurement of pulsating gas flows over a wide temperature range (at the moment from 20...450°C), such as found in the exhaust gas train of automotive combustion engines. Strong pressure fluctuations, high gas flow velocities, vortices in front of the transducers, and a wide temperature range, not only affect the signal-to-noise ratio (SNR), they also change and degrade the shape of the received signals.

With the major goal of realizing a transit time UFM, featuring high PRFs (several kHz range), we considered several state-of-the-art absolute transit time detection techniques, such as trigger level methods [2], pulse

compressed signals (chirp excitation) [7, 8], and cross-correlation techniques [9, 10]. However, pressure fluctuations, coherent multiple reflections between transmitting and receiving transducers [5], the requirement of high PRFs, and the lack of adequate reference signals for cross-correlation techniques when the signals change their shape, were the main motivation to develop an absolute transit time detection algorithm that is more tolerant of these issues.

The algorithm is based on using additional information from the phase domain for reproducible tracking. We use the Hilbert transform to calculate the phase signals (Fig. 1). Unlike previous published work [11], in which the unwrapped phase signal is calculated, we directly use the wrapped phase signal, which inherently divides the received time signal into sections, and thus helps finding the absolute transit times of the ultrasonic pulses step-by-step.

II. WORKING PRINCIPLE OF THE ALGORITHM

The ultrasonic transit time detection algorithm consists of nine main steps (Fig. 2):

Step 1: Using the measured temperature information of the gas in the flowmeter, an approximate time range, in which the arrival of the ultrasonic pulse is expected (trigger window), is determined.

Step 2: From this windowed time signal $y(t)$ the Hilbert transform $y_H(t)$ is calculated [Fig. 1(a)]. This can be done in the frequency domain by using a simple vector multiplication, *i.e.* with the transfer function of a Hilbert transformer ($-j \text{sign}(f)$).

Step 3: From $y(t)$ and $y_H(t)$, the wrapped phase signal [Fig. 1(b)] and the envelope [Fig. 1(a)] are calculated. The maximum of the envelope helps to find a local peak of one of the cycles, which is located in a more centered position [L_1 in Fig. 1(a)].

Step 4: The maximum of this local peak of $y(t)$ defines the starting point P_1 in the wrapped phase signal [Fig. 1(b)]. The other zero-crossing points ($P_{2...5}$) are found by searching in the phase vector. Because the ultrasonic pulse is limited in length, five points are sufficient. In the case of longer excitation signals this can be adapted accordingly. For the excitation of the transmitting transducers used in this study, we utilized a sinusoidal tone burst signal with a signal frequency of 350 kHz and a duration of three cycles.

Step 5: The wrapped phase signal [Fig. 1(b)] rotates uniformly from $-\pi$ to $+\pi$, with an almost constant slope, *i.e.* frequency, in the range where the received signal is present. This divides the signal into five regions (cycles),

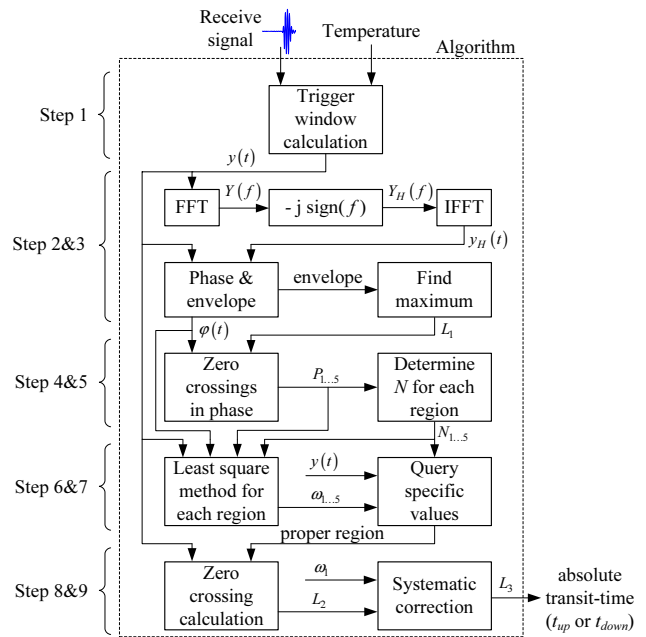


Fig. 2. Block diagram of the ultrasonic pulse arrival time detection algorithm (only one channel is shown).

each consisting of a specific number of phase sample points $N_{1...5}$ [Fig. 1(b)].

Step 6: Due to the almost constant slopes of the wrapped phase signal, a linear least squares method (LSM) can be employed to determine five straight lines, fitting through the phase points from one of the five phase data sets [Fig. 1(b)]. Each slope of these straight lines represents the local angular frequency ω for each cycle of the received signal, *i.e.* $\omega_{1...5}$. Note that we used broadband CUTs.

Step 7: The goal of this step is to find a characteristic local positive peak (second cycle of the pulse) of the received signal, in a reproducible way. By using information from the time and wrapped phase signal, the algorithm identifies one of the local positive peaks of the received signal, associated with one of the five zero-crossing points ($P_{1...5}$). This is done by comparing three values (local amplitude, number of phase sample points N , and angular frequency ω , *i.e.* time and phase domain characteristics are used) for each of the five cycles to the one corresponding to the cycle associated with P_1 . This is done step-by-step from the right to the left [Fig. 1(b)]. Only if all three values are within a given range (empirically determined), the first “significant” peak in the received signal is identified: The amplitude must exceed at least 70% of the amplitude obtained from step 3; the number N must exceed at least 70% of N_1 , obtained in step 5; and the deviation of the angular

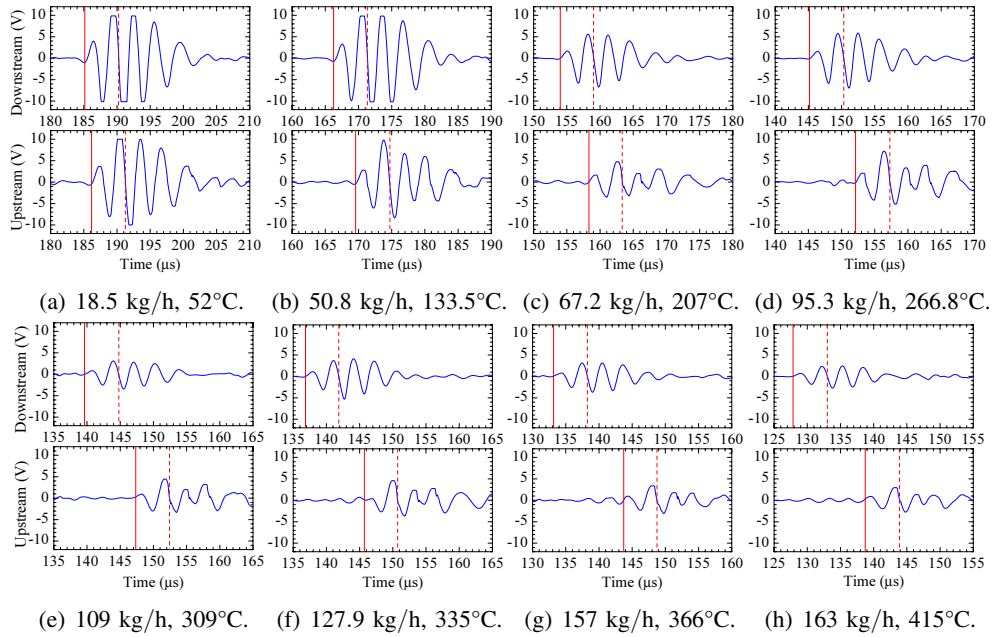


Fig. 3. Examples of received signals (downstream and upstream) for different gas mass flows and travel-path-averaged gas temperatures ((a)-(h)). The dashed vertical lines label the zero crossings L_2 , determined in step 8; the solid vertical lines the absolute transit times.

frequency ω must be within 2% of the angular frequency ω_1 .

Step 8: It may be argued that the zero crossings of the time signal are not much influenced by amplitude fluctuations, by signal shape distortions, and by noise in general. Thus, we use linear interpolation to determine the first zero-crossing point (L_2) after the local positive peak in the received signal found in step 7. The linear interpolation reduces the discrimination error $\pm \Delta t/2$, where Δt is the sample interval (we used 100 ns). This is outlined in the zoomed view in Fig. 1(a).

Step 9: Obviously L_2 does not mark the actual arrival time of the ultrasonic pulse. A systematic correction is required. By subtracting the time $\frac{3\pi}{\omega}$ from L_2 , where ω is the angular frequency of the first “significant” peak of the received signal obtained in step 7, we find the absolute transit time [L_3 , Fig. 1(a)] of the ultrasonic pulse.

III. RESULTS AND VERIFICATION

The detection algorithm was tested on real measurement data (Figs. 3(a)-(h)), obtained from a double-path UFM installed at the end of the exhaust gas train of an automotive combustion engine (4-cylinder gasoline direct injection (GDI) combustion engine from Adam Opel AG, Germany, with 2 liters displacement and an engine power of 80 kW). Details about the double-path UFM, the high-temperature resistant capacitive ultrasonic transducers [6], the calculation of the mass flow

values, and the method of using a temperature-dependent PRF to avoid problems associated with coherently reflected waves can be found in [5].

The engine load torque and engine speed were continuously increased, resulting in increasing gas mass flow values and travel-path-averaged gas temperatures. Higher gas temperatures result in higher sound velocities and therefore shorter transit times (Figs 3(a)-(h)). Stronger engine loads and higher gas flow velocities (up to 49 m/s, Mach number 0.1), increase pressure fluctuations, increase signal distortions, and reduce the SNR.

The PRFs ranged from 3 to 5 kHz [5]. For example, at a travel-path-averaged gas temperature of 415°C, ~ 4500 measurements per second were performed, allowing transient measurements of the exhaust gas mass flow.

For various engine conditions and over several time periods of one second each, both the downstream and upstream signals were recorded using a data acquisition board (PCI-6115, National Instruments Corporation). This enabled us to analyze the performance of the detection algorithm for each measurement. Over the mass flow range of 163 kg/h and gas temperature range of 400°C, corresponding to a SNR range from 18 to 8 dB, all signals were labelled correctly, *i.e.* without any cycle skip. No signal averaging was used.

The main outputs of the detection algorithm are the two absolute transit times (t_{down} , t_{up}), which are determined completely independent from each other. For

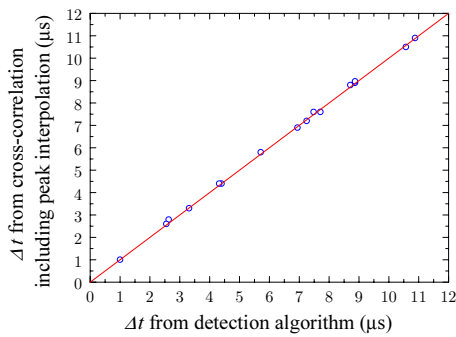


Fig. 4. Direct comparison between the relative time difference ($\Delta t = t_{up} - t_{down}$), calculated from the absolute transit times determined by the detection algorithm, and time difference using cross-correlation between the downstream and upstream signals with peak interpolation.

further verification of our results, we compared the calculated difference $\Delta t = t_{up} - t_{down}$ directly to a Δt , obtained by cross-correlation of the downstream and upstream signal. Peak interpolation of the normalized cross-correlation function was used to reduce the discrimination error [12]. For 16 different engine conditions in the same range as employed by Fig. 3, the relative average deviation was 0.78% ($\sigma = 1.79\%$) (Fig. 4).

Absolute transit time detection methods based on cross-correlation techniques require a stored reference signal that begins at time zero [10]. In applications where the signal shape changes, no such adequate reference signal can be found, even if stored for each channel independently. For example, if one uses the upstream signal from Fig. 3(a) with the determined absolute transit time of $185.17 \mu s$, one can shift this signal to time zero, *i.e.* it can be used as the reference signal for cross-correlation. However, due to the wide temperature range and strong pressure fluctuations in the exhaust gas train, the signal shapes change significantly (Fig.3). We observed large time errors, for example $2 \mu s$, if this hypothetical reference signal is cross-correlated with the upstream signal from Fig. 3(h).

IV. CONCLUSION

A reliable absolute transit time detection algorithm for UFM has been presented. In applications where the signal shapes change due to various parasitic influences such as temperature variations, pressure fluctuations, gas flow vortices, cross-talk in the electronics, etc., a reliable independent absolute transit time detection in each channel of the UFM is required. For pulsating gas flows, such as the exhaust gas train of an automotive combustion engine, using high PRFs is a main

requirement. To achieve this high PRF the excitation signal should be kept short, contradictory to compressed signal guidelines. Otherwise coherent reflections with long durations overlap with the main signal. Due to the lack of an adequate reference signal for these challenging UFM applications, cross-correlation methods are not suitable for the absolute transit time detection, but they can be used as an additional plausibility testing (at least for Δt) tool for the algorithm presented in this work. This will be part of future work.

ACKNOWLEDGMENT

This work was supported in part by AVL List GmbH, Graz, Austria. The authors would like to thank L. Lynnworth, Lynnworth Technical Services, Waltham, MA, for many fruitful discussions. The authors thank A. Schröder for fabricating the ultrasonic transducers used in this study.

REFERENCES

- [1] P. Hauptmann, N. Hoppe, and A. Püttmer “Review Article: Application of ultrasonic sensors in the process industry,” *Meas. Sci. Technol.*, vol. 13, pp. 73–83, 2002.
- [2] L. C. Lynnworth, *Ultrasonic Measurements for Process Control; Theory, Techniques, Applications*. San Diego: Academic Press, Inc., 1989.
- [3] L. C. Lynnworth, and Y. Liu *Ultrasonic flowmeters: Half-century progress report, 1955-2005*. *Ultrasonics*, vol. 44, pp. 1371–1378, 2006.
- [4] I. J. O’Sullivan and W. M. D. Wright, “Ultrasonic measurement of gas flow using electrostatic transducers,” *Ultrasonics*, vol. 40, pp. 407–411, 2002.
- [5] M. Kupnik, A. Schröder, P. O’Leary, E. Benes, and M. Gröschl, “Adaptive pulse repetition frequency technique for an ultrasonic transit time gas flowmeter for hot pulsating gases,” *IEEE Sensors Journal*, vol. 6, no. 4, pp. 906–915, 2006.
- [6] A. Schröder, S. Harasek, M. Kupnik, M. Wiesinger, E. Gornik, E. Benes, and M. Gröschl, “A capacitance ultrasonic transducer for high temperature applications,” *IEEE Trans. Ultrason., Ferroelect., Freq. Contr.*, vol. 51, pp. 896–907, 2004.
- [7] T. Folkestadt, and K. S. Mylvaganam, “Chirp excitation of ultrasonic probes and algorithm for filtering transit times in high-rangeability gas flow meters,” *IEEE Trans. Ultrason., Ferroelect., Freq. Contr.*, vol. 40, pp. 193–215, 1993.
- [8] J. Hossack “Introduction to IEEE TUFFC special issue on coded waveforms,” *IEEE Trans. Ultrason., Ferroelect., Freq. Contr.*, vol. 52, pp. 158–159, 2005.
- [9] S. A. Jacobson, L. C. Lynnworth, and J. M. Korba, *Differential correlation analyzer*. *US pat*, 4,787,252, 1988.
- [10] P. Brassier, B. Hosten, and F. Vulovic, “High-frequency transducers and correlation method to enhance ultrasonic gas flow metering,” *Flow Meas. Instr.*, vol. 12, pp. 201–211, 2001.
- [11] N. Roosnek, “Novel digital signal processing techniques for ultrasonic gas flow measurements,” *Flow Meas. Instr.*, vol. 11, pp. 89–99, 2000.
- [12] W. Q. Yang, and M. S. Beck, “An intelligent cross correlator for pipeline flow velocity measurement,” *Flow Meas. Instr.*, vol. 8, no. 2, pp. 77–84, 1997.